Autoimmunity

ISSN: 0891-6934 (Print) 1607-842X (Online) Journal homepage: http://www.tandfonline.com/loi/iaut20

Non-proliferating plasma cells detected in the salivary glands and bone marrow of autoimmune NOD.B10.H2b mice, a model for primary Sjögren's syndrome

Ewa A. Szyszko, Lara A. Aqrawi, Roland Jonsson, Karl A. Brokstad & Kathrine Skarstein

To cite this article: Ewa A. Szyszko, Lara A. Aqrawi, Roland Jonsson, Karl A. Brokstad & Kathrine Skarstein (2016) Non-proliferating plasma cells detected in the salivary glands and bone marrow of autoimmune NOD.B10.H2b mice, a model for primary Sjögren's syndrome, Autoimmunity, 49:1, 41-49, DOI: 10.3109/08916934.2015.1079820

To link to this article: http://dx.doi.org/10.3109/08916934.2015.1079820

Autoimmunity

http://informahealthcare.com/aut
ISSN: 0891-6934 (print), 1607-842X (electronic)

Autoimmunity, 2016; 49(1): 41–49
 DOI: 10.3109/08916934.2015.1079820

Taylor & Francis
Taylor & Francis Group

ORIGINAL ARTICLE

Non-proliferating plasma cells detected in the salivary glands and bone marrow of autoimmune NOD.B10.H2b mice, a model for primary Sjögren's syndrome

Ewa A. Szyszko[1,2], Lara A. Aqrawi[1], Roland Jonsson[1], Karl A. Brokstad[1], and Kathrine Skarstein[2,3]

[1]*Broegelmann Research Laboratory, Department of Clinical Science, University of Bergen, Bergen, Norway,* [2]*Gade Laboratory for Pathology, Department of Clinical Medicine, University of Bergen, Bergen, Norway, and* [3]*Department of Pathology, Haukeland University Hospital, Bergen, Norway*

Abstract

Autoantibody secreting plasma cells (PCs) are essential contributors in the development of autoimmune conditions such as primary Sjögren's syndrome (pSS). Particularly, the long-lived PC subset residing in the bone marrow has shown to continuously produce autoantibodies, whilst remaining unaffected by immunosuppressive treatment. We have previously shown accumulation of potentially long-lived PCs in chronically inflamed salivary glands of pSS patients. In this study, we aimed to characterise the PC compartment in the salivary glands (the target organ for pSS) and bone marrow before the onset of the murine pSS like disease versus advanced diseases progression. Bromodeoxyuridine (BrdU) was incorporated to distinguish the long-lived PCs. Double immunohistochemical staining and immunofluorescence were then conducted on submandibular gland and bone marrow sections from 8- and 40-week-old mice to identify BrdU and CD138. $BrdU^+$ cells were detected in the submandibular glands of 8-week-old mice, and observed within all focal infiltrates by 40 weeks of age. Most $CD138^+$ PCs were however $BrdU^-$ and located predominantly on the periphery of these infiltrates. This observation was verified through immunofluorescence. A comparable staining pattern was observed in the bone marrow of 8- and 40-week-old NOD.B10.H2b mice, where some of the $CD138^+$ cells also expressed BrdU. Interestingly, megakaryocytes in the bone marrow of NOD.B10.H2b mice were detected in close proximity to $CD138^+$ cells, illustrating a possible presence of PC survival niches. Our results demonstrate the presence and accumulation of potentially long-lived PCs in NOD.B10.H2b mice as the disease advances.

Keywords

Autoimmunity, NOD.B10.H2b mice, plasma cells, salivary glands, Sjögren's syndrome

History

Received 23 March 2015
Revised 8 July 2015
Accepted 2 August 2015
Published online 31 August 2015

Introduction

Sjögren's syndrome (SS) is a chronic autoimmune disease characterised by focal lymphocytic infiltration of exocrine glands, mainly salivary and lacrimal glands [1–4]. Due to difficulties in analysing early events of this disease in humans, several mouse models such as Murphy Roth's large (MRL) and non-obese diabetic (NOD) mice have been used in studying SS [5–10]. To date, the NOD mouse is one of the most used and thus best described out of these models. However, due to it developing diabetes the NOD strain is more appropriate for studying the secondary rather than primary form of SS. To overcome this problem, another congenic NOD strain has been developed, namely NOD.B10.H2b [11]. This novel strain exhibits all the immunopathological manifestations of the parental NOD mouse strain without the complication of diabetes. In consistence with human primary SS (pSS) patients, NOD.B10.H2b mice develop clinical signs such as loss of secretory function, and histological features such as lymphocytic infiltration of exocrine glands (lacrimal and salivary glands). The presence of hypergammaglobulinaemia and production of antinuclear autoantibodies (ANA) have also been disclosed in this model [12–14]. Taking all the aforementioned features into account, the NOD.B10.H2b mouse represents a promising model for the study of pSS.

SS is considered to be a B-cell driven disease [15–17]. High numbers of B cells accumulate in the salivary glands of SS patients, resulting in the development of B cell lymphoma in some instances [18]. B cell descendants, plasma cells (PCs) have been characterised as active players in SS [19]; they are the effector cells capable of producing autoantibodies against Ro/SSA and La/SSB self-antigens. Furthermore, a particular subtype of PCs, the long-lived PC subset that resides mainly in the bone marrow, have shown to produce autoantibodies without antigen stimulation, while remaining unaffected by

Correspondence: Prof. Kathrine Skarstein, Gade Laboratory for Pathology, Department of Clinical Medicine, University of Bergen, Haukeland University Hospital, N-5021 Bergen, Norway. Tel: +47 55 97 32 27. Fax: +47 55 97 31 58. E-mail: Kathrine.Skarstein@k1.uib.no

today's therapeutic approaches [20–22]. In addition to the bone marrow, PCs can also accumulate at site of inflammation, and have been shown to survive in the tissue until the inflammation dissolves with the support of specific survival signals [23]. As of today, little is known about the PC phenotypes in the target organs of SS patients and their possible role in disease pathogenesis. We have previously shown that potentially long-lived PCs accumulate in the minor salivary glands of pSS patients. These were non-proliferating cells that expressed high levels of anti-apoptotic B cell lymphoma 2 (Bcl2) protein [24]. Moreover, the expression of factors necessary for PC survival in both the salivary glands [24] and peripheral blood [25] of pSS patients has also been accounted for earlier.

In the present study, we aimed to perform a descriptive histopathological characterisation of the PC compartment in the salivary glands and bone marrow of NOD.B10.H2b mice in order to gain better insight in disease pathogenesis. Following the incorporation of bromodeoxyuridine (BrdU), double immunohistochemical staining of both paraffin-embedded and frozen tissue sections from 8- and 40-week-old diseased mice were performed using BrdU and CD138 monoclonal antibodies. Taking into account our previous findings on the identification of distinct phenotypes of PCs in the spleen and bone marrow of NOD.B10.H2b mice via flow cytometry [26], our recent results further demonstrate the presence of both short- and long-lived PCs residing in the submandibular glands and bone marrow of the autoimmune NOD.B10.H2b mouse, with an accumulation of long-lived PCs in the submandibular glands as the disease progresses. Additionally, the detection of megakaryocytes in the bone marrow in close proximity to $CD138^+$ cells illustrates a possible presence of survival niches that propagate essential PC survival signals. Although, further investigation of the bone marrow microenvironment is needed to confirm this conception.

Material and methods

Mice and BrdU treatment

Female NOD.B10H2b mice and BALB/c mice were purchased from Jackson Laboratories (Bar Harbor, ME) and Taconic (Ry, Denmark) respectively. The mice were divided into two age groups (8 and 40 weeks) with 10 NOD.B10.H2b and 8 BALB/c mice included in each group. Eleven days before sacrifice, the mice were treated with BrdU in drinking water (0.8 mg/ml) on a daily basis, where the BrdU solution was protected from light and changed every other day. This study was approved by the National Animal Research Authority of Norway (#2006014BB).

Stimulated saliva collection

Stimulated saliva was collected from both NOD.B10.H2b and BALB/c mice as described previously [26]. In brief, a day before sacrifice, each mouse was weighed and treated with Ketalar (0.75 mg/100 g body weight) and Dormitor (0.01 mg/100 g body weight) dissolved in phosphate-buffered saline (PBS). Salivary flow was stimulated by an intraperitoneal injection of pilocarpine (0.05 mg/100 g of body weight) and saliva was collected with a micropipette for 10 min. The volume of each sample was calculated, and the salivary flow was represented as saliva volume/body weight (μl/g).

Salivary gland and bone collection

Mice were euthanized by CO_2 asphyxiation, and salivary glands (submandibular, sublingual and parotid glands) were dissected along with the spinal and humerus bones. The salivary glands were fixed in formalin and embedded in paraffin, while the bones were first fixed in formalin and then placed in decalcification medium containing ethylenediaminetetraacetate (EDTA) and polyvinylpyrrolidone (PVP). A Leica serial microtome (Leica Instruments GmbH, Nussloch, Germany) was used to section the samples [submandibular gland (SG) 4–6 μM thick, BM 2 μM thick]. Haematoxylin and eosin (H&E) staining was then performed to determine the degree of inflammation, where the sections were then analysed and evaluated as described below.

Primary antibodies

The following primary anti-mouse antibodies were used in this study at the indicated dilution: rat anti-mouse CD138 (SG 1:3000, BM 1:200) (clone 281-2, BD Biosciences, San Jose, CA), mouse anti-BrdU (1:10) (BD Biosciences, San Diego, CA), rat anti-PNAd (clone MECA-79, BD Biosciences, San Jose, CA) and rabbit anti-mouse CD27 (clone EPR8569, Abcam, Cambridge, UK).

Immunohistochemistry

Single-staining

Single immunohistochemical staining was performed by Avidin Biotin Complex (ABC) method as described previously [27]. In short, the paraffin-embedded, formalin-fixed submandibular gland tissue sections were placed on SuperFrost® Plus microscope slides (Fisher Scientific, Pittsburgh, PA) and incubated overnight in a heat cabinet at 56 °C. This was followed by deparaffinisation in xylene, and rehydration through a graded ethanol series (100%, 96%, 70%) and distilled water. The sections were then subjected to heat-induced epitope retrieval (HIER) with citrate buffer (Target Retrieval Solution, pH 6.0, BD Biosciences, San Diego, CA), and blocking with avidin and biotin (Vector Blocking Kit, SP2001, Vector Laboratories, Burlingame, CA) for 15 min each. The peroxidase activity was also blocked for 10 min (Peroxidase Blocking Solution, S2023, Dako, Glostrup, Denmark) followed by Tris-buffered saline (TBS) containing 10% rabbit serum (X0902, Dako, Glostrup, Denmark) and 3% bovine serum albumin (BSA) (Sigma-Aldrich, Oslo, Norway) for 30 min. The sections were then incubated with primary antibody (CD138 and PNAd) diluted in antibody diluent (S0809, Dako, Glostrup, Denmark) for 60 min. This was followed by incubation with biotinylated rabbit anti-rat secondary antibody (E0468, Dako, Glostrup, Denmark) for 30 min, and then ABC (Vectastain ABC kit, Vector Laboratories, Burlingame, CA) for another 30 min. Thereafter, the sections were incubated for 10 min with diaminobenzidine (DAB), which was used as chromogen for development (K4007, Dako, Carpentaria, CA). All

incubations were performed at room temperature (RT), and TBS containing 0.1% Tween (TBST) was used as washing buffer (pH 7.6) between every step for 10 min. Finally, the sections were counterstained with Haematoxylin (S3301, Dako) for 4 min, dehydrated using ethanol (70%, 96%, 100%) and xylene, and mounted in Eukitt (O. Kindler GmbH & Co, Freiburg, Germany).

Double-staining

Expression of BrdU and CD138 was detected by double-staining of sections from both the submandibular gland and bone marrow using BrdU In-Situ Detection Kit (BD Biosciences, San Jose, CA). In short, the sections were pre-treated as previously described following the procedure in the single-staining, using retrieval solution, pH 6.0 (BD Biosciences, San Jose, CA) for antigen retrieval and peroxidase activity was blocked for 10 min. The first primary antibody (BrdU) was then added and the sections were incubated for 60 min at RT. Thereafter, incubation with streptavidin-horseradish peroxidase (HRP) enzyme complex (BD Biosciences, San Jose, CA) was performed for 30 min. DAB was used as substrate for visualising the staining of BrdU in submandibular gland sections and in the bone marrow. Following this, the sections were rinsed in tap water for 5 min and in TBST for 10 min. Then the sections were incubated with the second primary antibody (CD138) for 60 min at RT, and placed at 4 °C overnight. Similar to the single-staining procedure, binding of the second primary antibody was detected by incubation with biotinylated anti-rat antibody, followed by alkaline phosphatase, (AK-5001, Vectastain ABC kit) for 30 min. As a chromogen, sections were incubated with Liquid Permanent Red (LPR) (K0640, Dako, Carpentaria, CA) for 15 min. As described above, the sections were washed in TBST for 10 min between every step, and consecutively counterstained with Haematoxylin, then dehydrated, and mounted in Eukitt.

Immunofluorescence

Immunoflourescent staining was performed on submandibular gland tissue to visualise whether $CD138^+$ cells were proliferating and thus also expressing BrdU. The single ABC method was used, as described above. However, staining was developed with secondary antibodies conjugated to AlexaFlour 448 (green) for CD138, and AlexaFlour 594 (red) for BrdU. The sections were then counterstained with DAPI (blue).

Evaluation of staining

All sections were studied using a light microscope (Leica, DMLB, Leica Microsystems Wetzlar, Wetzlar) by three investigators. Submandibular salivary gland tissue samples were evaluated by morphometric analysis of the sections; through connecting the light microscope to a Color View III-camera and AnalySIS software (Soft Imaging System GmbH) to determine the focus score (FS). This was defined as the number of foci of 50 or more mononuclear cells per mm^2 of glandular tissue, as performed previously [28]. Both mononuclear cells in focal infiltrates and those located interstitially i.e. in close proximity to the acinar or ductal epithelium were analysed. Histology of bones was also determined by morphological examination of H&E stained sections. Cells were considered positive when 50% or more of the cell membrane was positively stained with the consecutive antibodies in both the submandibular glands and bone marrow.

Statistical analysis

Statistical significance was evaluated by the Student's *t*-test and the Wilcoxon-signed Rank Test. Values were presented as mean where differences were considered significant when $p \leq 0.05$. In addition, the Pearson correlation test was used to examine the association between the different parameters.

Results and discussion

Histopathological changes in the salivary glands of NOD.B10.H2b mice

H&E sections from submandibular glands of NOD.B10.H2b and BALB/c mice were examined and the FS was evaluated. Only scattered mononuclear cells were observed in the 8-week-old NOD.B10.H2b mice, and none of the observed cell aggregates consisted of >50 mononuclear cells, thereby resulting in an FS value of 0. In the 40-week-old mice, a significant increase in number of foci was observed (mean FS of 0.3, $p \leq 0.02$). Meanwhile, no focal inflammation of submandibular glands was observed in both 8 and 40-week-old control BALB/c mice (data not shown). Furthermore, salivary flow was also measured and presented as stimulated salivary flow rate [µl saliva/g body weight] in both NOD.B10.H2b and BALB/c mice. There was a significant decrease in salivary flow in the 40-week-old NOD.B10.H2b mice compared to the 8-week-old mice ($p \leq 0.0002$) (Figure 1A). The BALB/c mice, on the other hand, exhibited an increase in salivary flow from 8 weeks (1.62 µl/g salivary flow mean) to 40 weeks (4.28 µl/g salivary flow mean) (data not shown). Similar to disease development in pSS patients, combined, our results demonstrate how disease progression in the autoimmune NOD.B10.H2b mouse results in an increase in FS of the salivary glands and a decrease in salivary flow, in turn leading to the common symptoms of dry mouth. Moreover, these observations further demonstrate how the NOD.B10.H2b mouse represents a promising model for the study of pSS.

In general, we observed focal mononuclear cell infiltration in submandibular, sublingual and parotid glands of 40-week-old NOD.B10.H2 mice (Figure 1B). However, the submandibular glands were the most affected ones, with the highest numbers of foci per glandular tissue area observed. In our experiment, apparent focal inflammation of the submandibular glands was detected primarily at 40 weeks of age in the NOD.B10.H2 mice, whereas at 24 weeks only a few animals had focal inflammation in their submandibular gland tissue (data not shown). On the other hand, comparable FS could already be observed in NOD mice at Week 17 [5,11,29]. Evidently, the differences between the NOD mouse and its congenic NOD.B10.H2b strain are more than presence or lack of diabetes, as the disease onset and progression can also vary. Furthermore, a previous study on the NOD.B10.H2b model

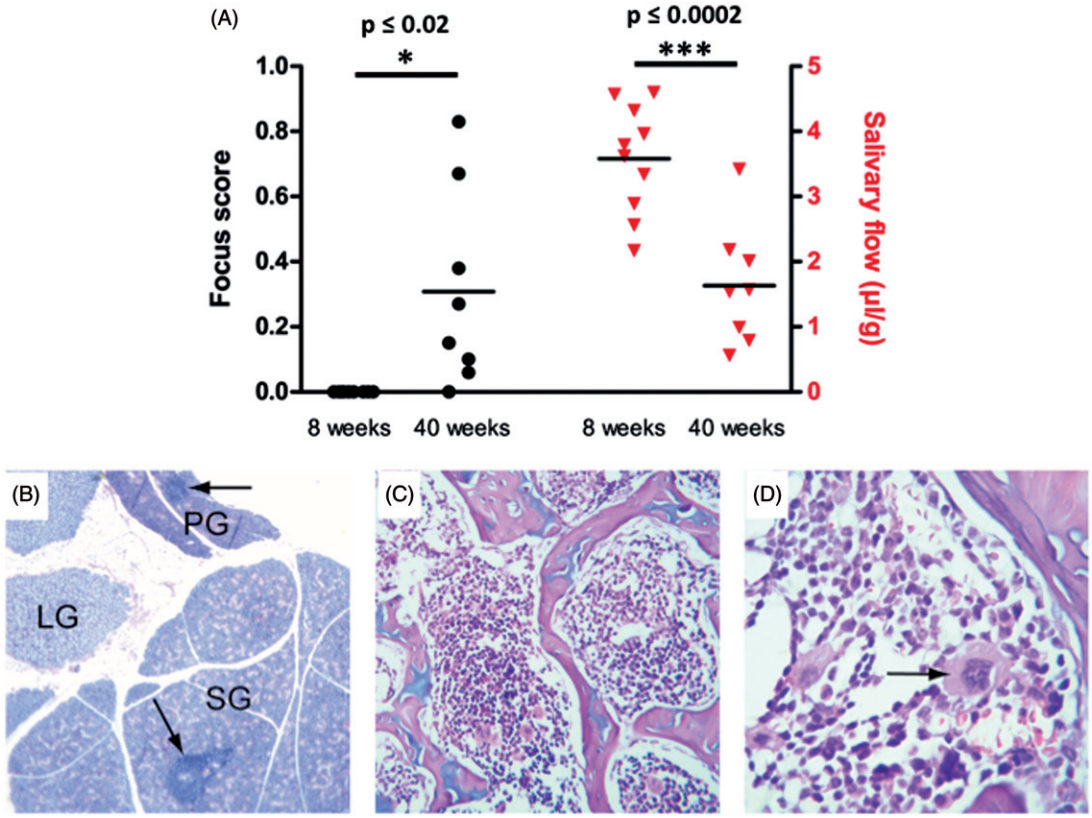

Figure 1. FS, salivary flow and histopathology of salivary glands and bone marrow in NOD.B10.H2b mice. (A) FS, represented by black circles, is defined as the number of foci comprising >50 mononuclear cells per mm^2 of submandibular glands in 8- and 40-week-old NOD.B10.H2b mice. There is a significant increase in the FS of 40-week-old mice compared to the 8-week-old ($p \leq 0.02$). No focal infiltration of mononuclear cells is detected in the submandibular glands of BALB/c mice (data not shown). Salivary flow, represented by red triangles, is presented as stimulated salivary flow rate [µl saliva/g body weight] in 8- and 40-week-old NOD.B10.H2b mice. There is a significant decrease in salivary flow in the 40-week-old NOD.B10.H2b mice compared to the 8-week-old mice ($p \leq 0.0002$). Meanwhile, in BALB/c mice the salivary flow increased significantly from 8 weeks (1.62 µl/g salivary flow mean) to 40 weeks (4.28 µl/g salivary flow mean) (data not shown). (B) Tissue section from a 40-week-old NOD.B10.H2b mouse showing parts of SG: submandibular gland, PG: parotid gland and LG: sublingual gland. Presence of focal mononuclear cell infiltration (arrows) are found in all types of glands, here shown in SG and PG. (C) H&E section of bone marrow from a 40-week-old NOD.B10.H2b mouse showing blasts and progenitor lymphoid cells (D) Higher magnification of a bone marrow section showing megakaryocytes with large polymorph nuclear cells, as indicated by arrow.

detected inflammation in the submandibular glands already at 24 weeks of age [14]. This underlines the importance and potential influence the environment has on development of disease in experimental models.

Characterisation of the bone marrow in NOD.B10.H2b mice

Since long-lived PCs have been shown to reside predominantly in the bone marrow [30–32] we wished to characterise the bone marrow compartment of the NOD.B10.H2b and BALB/c mice. Hence, the spine and the humerus bone were collected and decalcified [33]. Bones were then paraffin-embedded and the H&E sections were analysed (Figure 1C and D). By morphology, we observed occurrence of lymphoid cells, granulocytes such as eosinophils and neutrophils, and megakaryocytes in both mouse strains. Interestingly, megakaryocytes have been characterised as functional components of PC survival niches [34–36] that propagate essential signals for cell survival through direct interaction with the PCs [23,37]. Examples of such survival factors include a proliferation-inducing ligand (APRIL) and interleukin-6 (IL-6). We have previously characterised the expression of these survival factors in both the minor salivary glands [24] and peripheral blood [25] of pSS patients. Furthermore, we have also verified the expression of Protein NH2-Terminal Asparagine Deamidase (PNAd); a marker expressed on high endothelial venules, in the submandibular glands and lymph nodes of our NOD.B10.H2b model (Supplementary Figure 1). These $PNAd^+$ specialised vessels promote the migration of lymphocytes to secondary lymphoid organs, and have also been associated to lymphoid neogenesis in autoimmune diseases (including SS) and accompanying mouse models [7,38–41]. Consequently, the detection of megakaryocytes in the bone marrow of our studied mouse strain is an additional implication of this.

$CD138^+$ PCs in salivary glands and bone marrow of NOD.B10.H2b mice

Haven already accounted for the phenotypic diversity of PCs in the spleen and bone marrow of NOD.B10.H2b mice via flow cytometry previously [26], we wished to further characterise the PC pattern in the submandibular glands and bone marrow of these mice using single CD138 immunohistochemical staining. We have previously detected high amounts of PCs accumulating in the minor salivary glands of pSS patients [24]. However, different PC distribution

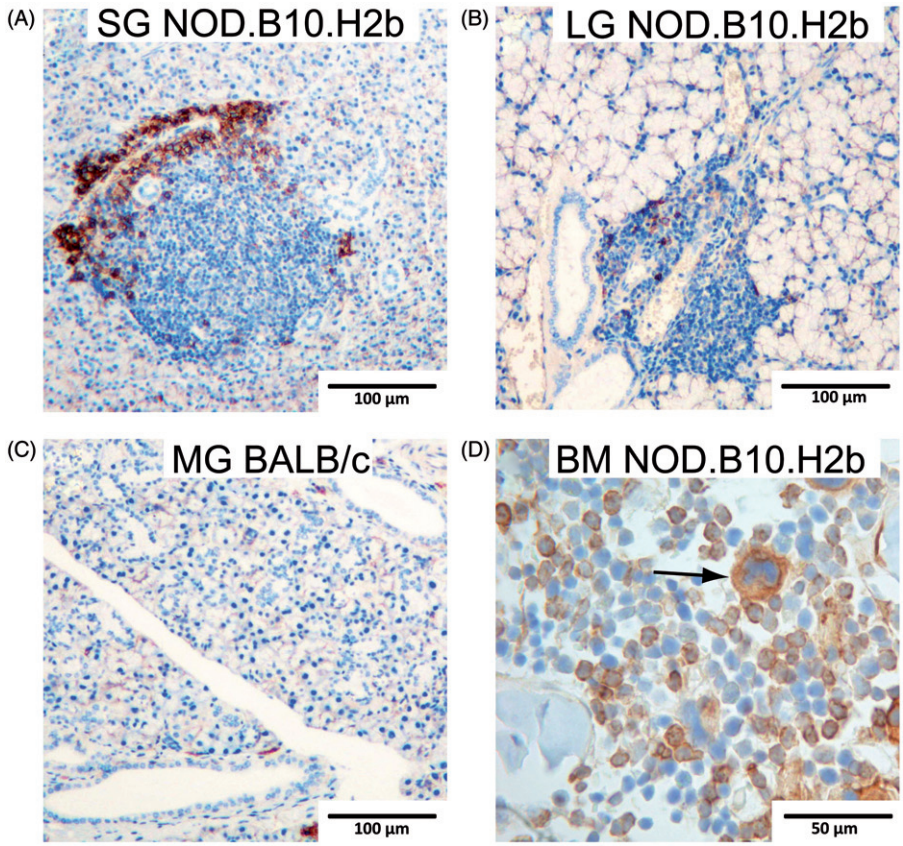

Figure 2. CD138$^+$ PCs in salivary glands and bone marrow of NOD.B10.H2b mice. (A) CD138$^+$ PCs are mainly located in the periphery of mononuclear infiltrates in the submandibular salivary gland (SG) tissue of 40-week-old NOD.B10.H2b mice. CD138$^+$ PCs are also commonly detected in interstitial areas. (B) In the sublingual glands (LG), CD138$^+$ PCs are detected in the focal infiltrates of 40-week-old NOD.B10.H2b mice. (C) CD138$^+$ PCs are also seen scattered in the interstitial areas of SG from 40-week-old BALB/c mice. (D) CD138$^+$ staining of bone marrow cells in 40-week-old NOD.B10.H2b mice, showing a large megakaryocyte with a polymorph nucleus in close proximity to CD138+ PCs (as indicated by arrow).

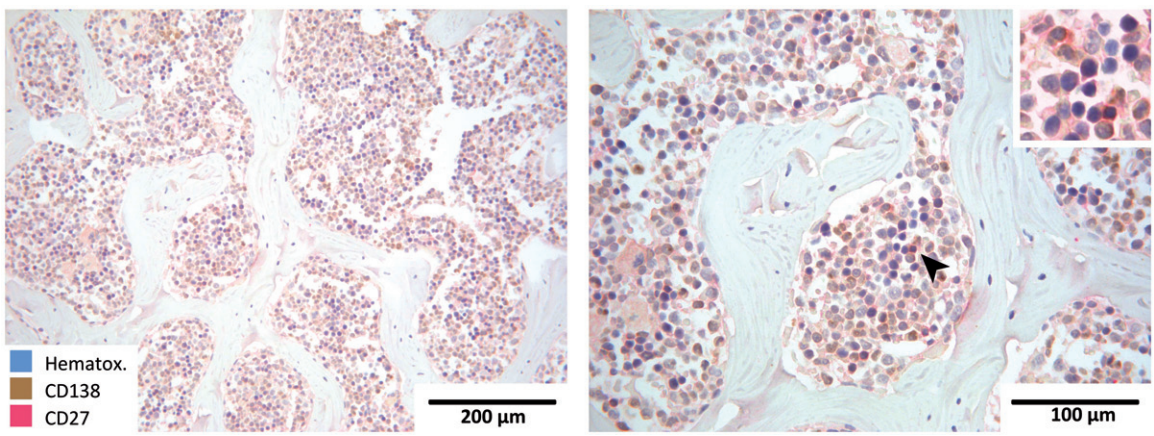

Figure 3. CD138 and CD27 expression pattern in the bone marrow of NOD.B10.H2b mice. Double immunohistochemical staining performed in the bone marrow to further examine the expression of CD138 (brown) in relation to CD27$^+$ cells (red). Most of the CD138$^+$ cells are single-positive (brown), and only a few double-positive CD27$^+$/CD138$^+$ cells are observed, verifying that most of these CD138 positive cells belong to the long-lived PC subset.

patterns were found in the submandibular glands of NOD.B10.H2b mice.

Only few CD138$^+$ PCs were observed in the interstitial areas of submandibular salivary gland tissue of 8-week-old NOD.B10.H2b mice, while increased numbers of CD138$^+$ cells were detected in the submandibular glands of 40-week-old mice. Similar to our observations when staining for CD138+ cells in the minor salivary glands of pSS patients [24,42], these PCs were mainly located in the periphery of focal infiltrates, with a few CD138$^+$ cells found in the interstitium (Figure 2A). However, in the sublingual tissue of NOD.B10.H2b mice, CD138$^+$ cells were mainly detected in the central area of focal infiltrates (Figure 2B). No CD138$^+$ PCs were observed in any of the submandibular glands of 8-week-old BALB/c mice. Still, a few CD138$^+$ PCs were detected in these mice at 40 weeks of age (Figure 2C).

Examination of bone marrow sections from NOD.B10.H2b mice revealed positive CD138 staining on a range of cells (Figure 2D). Notably, CD138 expression was also detected on megakaryocytes in close proximity to the CD138$^+$ cells. By morphology we determined some of these cells being PCs. However, CD138 can be expressed on both pre-B cells and

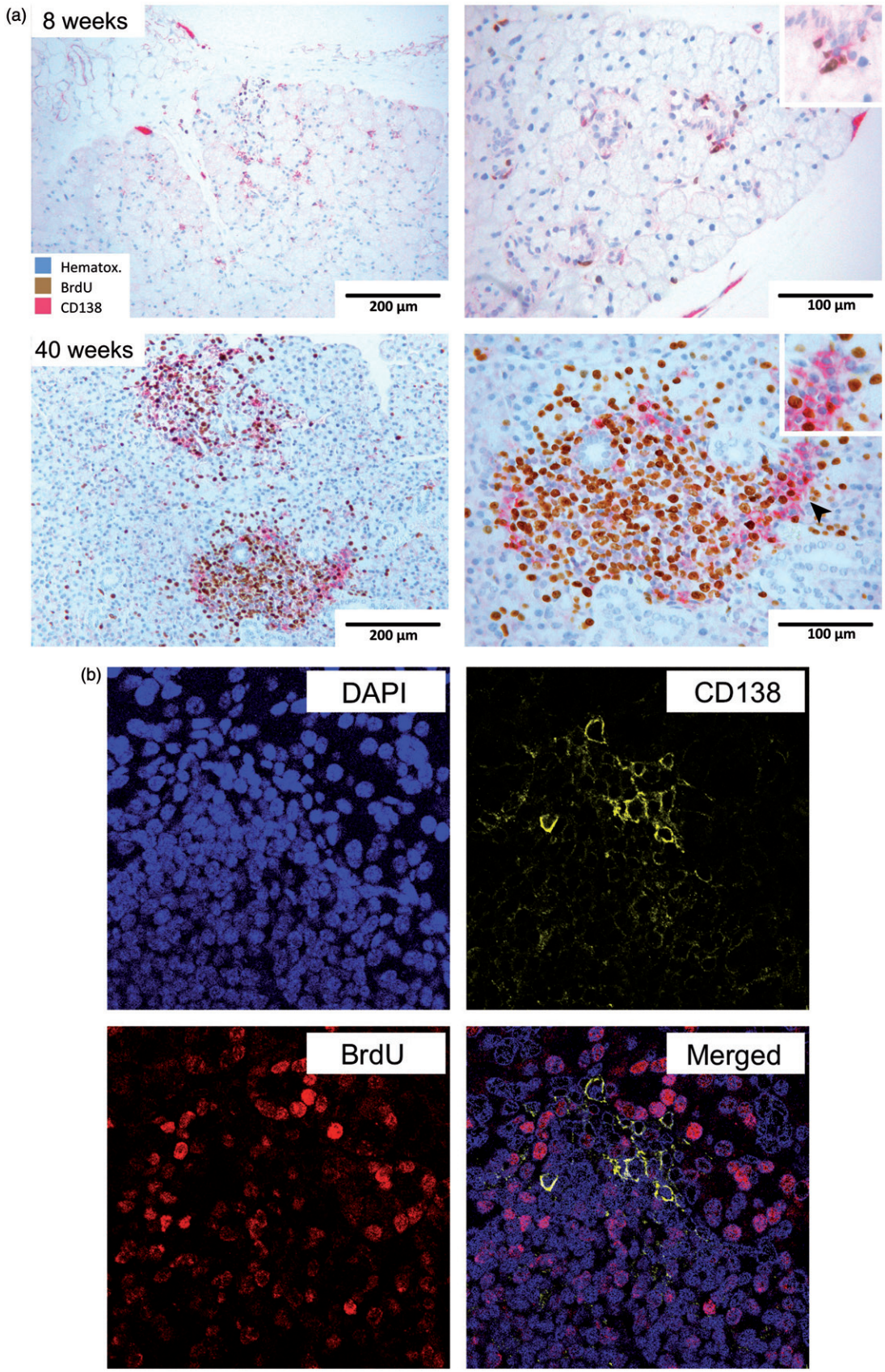

Figure 4. CD138 and BrdU expression pattern in the salivary glands of NOD.B10.H2b mice. (A) Double-staining of BrdU (brown) and CD138 (red) on formalin-fixed, paraffin-embedded sections of submandibular glands of 8-week-old and 40-week-old NOD.B10.H2b mice. Scattered single-positive BrdU cells (brown) can be seen in the submandibular glands of 8-week-old NOD.B10.H2b mice, while some are also $BrdU^{+}/CD138^{+}$, indicating the presence of short-lived PCs. A few single-positive CD138 cells (red) are also observed, signifying the detection of long-lived PCs already at early age. Increased numbers of BrdU+ cells (brown) are observed within all focal infiltrates in 40-week-old autoimmune mice. The CD138+ cells are observed primarily in the periphery of these focal infiltrates, and are mostly $BrdU^{-}$, signifying long-lived PCs (as indicated by arrow and a higher magnification in the upper right corner). (B) Immunofluorescent CD138 membrane staining detected with Alexa-Fluor 488 (green), and BrdU nuclear staining identified with Alexa-Fluor 594 (red). General nuclear staining is detected with DAPI (blue). An overlay shows that some $CD138^{+}$ cells present in the submandibular glands of 40-week-old NOD.B10.H2b mice are $BrdU^{-}$, and thus a possible candidate for the long-lived PC subset.

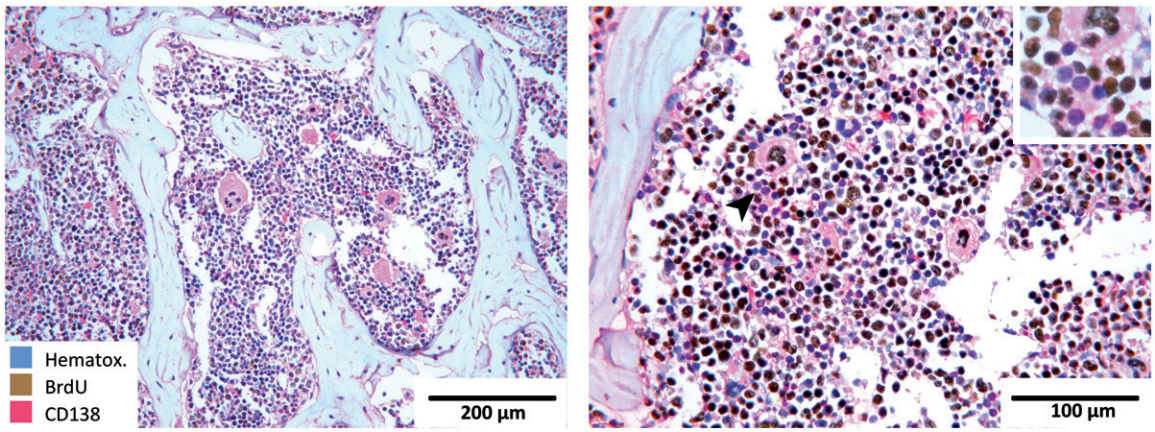

Figure 5. CD138 and BrdU expression pattern in the bone marrow of NOD.B10.H2b mice. Double immunohistochemical staining performed in the bone marrow to further examine the incorporation of BrdU (brown) in relation to $CD138^+$ cells (red). A comparable staining pattern is observed for both the 8-week-old and 40-week-old NOD.B10.H2b mice, where some of the $CD138^+$ cells also express BrdU, while single-positive cells expressing either CD138 (red) or BrdU (brown) are also detected. Interestingly, some of these $CD138^+$ single stained cells (red) are observed in close proximity to the megakaryocytes (as indicated by arrow and a higher magnification in the upper right corner). The figure shows a bone marrow section from an 8-week-old mouse.

PCs in mice [43], both of which are found in the bone marrow. This is why an additional double-staining experiment was performed for verification, where we stained for CD27 alongside CD138. As predicted, most of the $CD138^+$ cells were negative for CD27, and only a few double-positive $CD27^+/CD138^+$ cells were observed (Figure 3). As CD27 is a marker for differentiating B cells in mouse (centrocytes) [44,45] the detection of these single-positive $CD138^+$ cells implies that they are not in the process of differentiation. A similar staining was observed in the bone marrow of BALB/c mice (data not shown).

It has been presented by Winter et al. [34] that in the murine bone marrow PCs reside in close proximity to and interact with megakaryocytes. By morphology, we observed both $CD138^+$ PCs together with other $CD138^+$ lymphoid cells in the vicinity of these megakaryocytes, thus indicating the possible impact of megakaryocytes on survival of both PCs and pre-B cells found in the bone marrow. However, further investigation is needed to confirm this notion.

CD138 and BrdU expression pattern in the salivary glands and bone marrow of NOD.B10.H2b mice

We have previously shown that high proliferative activity could be observed in the minor salivary glands of pSS patients through the immunohistochemical staining of Ki-67, a nuclear protein associated with cellular proliferation, alongside CD138 [24]. This is why we wished to study the proliferation pattern of PCs both early and late in the disease development using the NOD.B10.H2b model. These autoimmune mice were therefore treated with BrdU in drinking water. BrdU incorporation by PCs was examined through double immunohistochemical staining of BrdU alongside CD138 in salivary glands, which was verified further by immunoflourescent staining. As it has been shown that long-lived PCs residing in the murine bone marrow are non-proliferating cells with low metabolic activity [23,46], additional double immunohistochemical staining was performed in the bone marrow to further examine the incorporation of BrdU in relation to $CD138^+$ cells.

Low metabolic activity could already be detected in the submandibular glands of 8-week-old NOD.B10.H2b mice, where scattered single-positive BrdU cells could be observed, while some are also $BrdU^+/CD138^+$, indicating the presence of short-lived PCs. A few single-positive CD138 cells were also observed, signifying the detection of long-lived PCs already at early age and an early stage of the disease present in the target organ. This proliferative and metabolic activity increased with age, as we observed higher amounts of $BrdU^+$ cells within all focal infiltrates in the 40-week-old autoimmune mice. Also, this double-staining of CD138 with BrdU revealed that these $CD138^+$ cells detected were mostly $BrdU^-$, with the $CD138^+$ cells located predominantly on the periphery of the focal infiltrates (Figure 4A). No proliferative activity was detected in the submandibular glands of any of the BALB/c mice (data not shown). Nevertheless, comparable single BrdU staining was observed in the lymph nodes of both NOD.B10.H2b and BALB/c mice (data not shown). Moreover, the verification with immunoflourescent staining using antibodies against CD138 and BrdU showed how similar to the situation observed in human minor salivary glands [24], certain PCs in submandibular glands of autoimmune mice were inactive and non-proliferating PCs (Figure 4B), thus a possible candidate for the long-lived subset [46]. The detection of this long-lived subset of PCs in the target organ of these diseased mice could explain the continuous autoantibody production at the site of inflammation [47]. This might also have a consequence for the resistance to the anti-CD20 targeted therapy that does not target the CD20 negative PCs.

In the bone marrow, on the other hand, a comparable staining pattern was observed for both the 8-week-old and 40-week-old NOD.B10.H2b mice, where some of the $CD138^+$ cells also incorporated BrdU, while single-positive cells were also observed for each CD138 and BrdU, respectively (Figure 5). This is in contrast to what was observed in the submandibular gland, where the proliferative and metabolic activity increased with age as the disease advanced. Nonetheless, the identification of $CD138^+$ cells in the bone

marrow of NOD.B10.H2b mice that are $BrdU^{-}$ illustrates the possible presence of long-lived PCs in both age groups. A further examination of the bone marrow microenvironment could reveal whether the autoimmune NOD.B10.H2b mouse comprises the necessary survival niches for these long-lived PCs.

Conclusions

Our results demonstrate that there are possible candidates for a long-lived PC subset in the submandibular glands and bone marrow of the autoimmune NOD.B10.H2b model that accumulates in the submandibular glands as the disease develops. Moreover, the detection of megakaryocytes in close proximity to $CD138^{+}$ cells in the bone marrow shows a possible presence of survival niches that provide essential PC survival signals. However, whether the NOD.B10.H2b mouse truly comprises the necessary survival niches for these long-lived PCs found in pSS patients requires a further investigation of the bone marrow microenvironment. Still, our current findings provide additional insight in understanding the limitations of present therapeutic strategies in SS that target CD20+ cells, while this long-lived PC subset residing in target organs remains unaffected by treatment.

Acknowledgements

We gratefully acknowledge Edith Fick, Kjerstin Jakobsen, Gunnvor Øijordsbakken and Marianne Eidsheim for excellent technical assistance.

Declaration of interest

The authors report no conflicts of interest. The authors alone are responsible for the content and writing of this article.

This study was supported by the Faculty of Medicine and Dentistry at the University of Bergen, the L. Meltzer Foundation, the Strategic Research Program at Helse Bergen, the Western Regional Health Authority and the Broegelmann Foundation.

References

1. Jonsson, R., A. I. Bolstad, K. A. Brokstad, and J. G. Brun. 2007. Sjogren's syndrome – a plethora of clinical and immunological phenotypes with a complex genetic background. *Ann. NY Acad. Sci*. 1108: 433–447.
2. Jonsson, R., P. Vogelsang, R. Volchenkov, et al. 2011. The complexity of Sjogren's syndrome: novel aspects on pathogenesis. *Immunol. Lett*. 141: 1–9.
3. Kassan, S. S., and H. M. Moutsopoulos. 2004. Clinical manifestations and early diagnosis of Sjogren syndrome. *Arch. Intern. Med*. 164: 1275–1284.
4. Mavragani, C. P., and H. M. Moutsopoulos. 2014. Sjogren's Syndrome. *Annu. Rev. Pathol*. 9: 273–285.
5. Gao, J., S. Killedar, J. G. Cornelius, et al. 2006. Sjogren's syndrome in the NOD mouse model is an interleukin-4 time-dependent, antibody isotype-specific autoimmune disease. *J. Autoimmun*. 26: 90–103.
6. Hoffman, R. W., M. A. Alspaugh, K. S. Waggie, et al. 1984. Sjogren's syndrome in MRL/l and MRL/n mice. *Arthritis. Rheum*. 27: 157–165.
7. Jonsson, M. V., N. Delaleu, and R. Jonsson. 2007. Animal models of Sjogren's syndrome. *Clin. Rev. Allergy Immunol*. 32: 215–24.
8. Kunkel, E. J., and E. C. Butcher. 2003. Plasma-cell homing. *Nat. Rev. Immunol*. 3: 822–829.
9. Skarstein, K., M. Wahren, E. Zaura, et al. 1995. Characterization of T cell receptor repertoire and anti-Ro/SSA autoantibodies in relation to sialadenitis of NOD mice. *Autoimmunity.* 22: 9–16.
10. Kessler H. S. 1968. A laboratory model for Sjogren's syndrome. *Am. J. Pathol*. 52: 671–685.
11. Robinson, C. P., S. Yamachika, D. I. Bounous, et al. 1998. A novel NOD-derived murine model of primary Sjogren's syndrome. *Arthritis. Rheum*. 41: 150–156.
12. Humphreys-Beher, M. G., Y. Hu, Y. Nakagawa, et al. 1994. Utilization of the non-obese diabetic (NOD) mouse as an animal model for the study of secondary Sjogren's syndrome. *Adv. Exp. Med. Biol*. 350: 631–636.
13. Wicker, L. S., B. J. Miller, L. Z. Coker, et al. 1987. Genetic control of diabetes and insulitis in the nonobese diabetic (NOD) mouse. *J. Exp. Med*. 165: 1639–1654.
14. Nguyen, C., J. Cornelius, E. Singson, et al. 2006. Role of complement and B lymphocytes in Sjogren's syndrome-like autoimmune exocrinopathy of NOD.B10-H2b mice. *Mol. Immunol*. 43: 1332–1339.
15. Jonsson, R., E. Nginamau, and K. A Szyszko. 2007. Brokstad. Role of B cells in Sjogren's syndrome – from benign lymphoproliferation to overt malignancy. *Front. Biosci*. 12: 2159–2170.
16. Pers, J. O., and P. Youinou. 2013. Are the B cells cast with the leading part in the Sjogren's syndrome scenario? *Oral Dis*. 20: 529–537.
17. Youinou, P., V. Devauchelle-Pensec, and J. O. Pers. 2010. Significance of B cells and B cell clonality in Sjogren's syndrome. *Arthritis. Rheum*. 62: 2605–2610.
18. Pollard, R. P., J. Pijpe, H. Bootsma, et al. 2011. Treatment of mucosa-associated lymphoid tissue lymphoma in Sjogren's syndrome: a retrospective clinical study. *J. Rheumatol*. 38: 2198–2208.
19. Szyszko, E. A., J. G. Brun, K. Skarstein, et al. 2011. Phenotypic diversity of peripheral blood plasma cells in primary Sjogren's syndrome. *Scand. J. Immunol*. 73: 18–28.
20. Manz, R. A., M. Lohning, G. Cassese, et al. 1998. Survival of long-lived plasma cells is independent of antigen. *Int. Immunol*. 10: 1703–1711.
21. Vallerskog, T., I. Gunnarsson, M. Widhe, et al. 2007. Treatment with rituximab affects both the cellular and the humoral arm of the immune system in patients with SLE. *Clin. Immunol*. 122: 62–74.
22. DiLillo, D. J., Y. Hamaguchi, Y. Ueda, et al. 2008. Maintenance of long-lived plasma cells and serological memory despite mature and memory B cell depletion during CD20 immunotherapy in mice. *J. Immunol*. 180: 361–371.
23. Cassese, G., S. Arce, A. E. Hauser, et al. 2003. Plasma cell survival is mediated by synergistic effects of cytokines and adhesion-dependent signals. *J. Immunol*. 171: 1684–1690.
24. Szyszko, E. A., K. A. Brokstad, G. Oijordsbakken, et al. 2011. Salivary glands of primary Sjogren's syndrome patients express factors vital for plasma cell survival. *Arthritis. Res. Ther*. 13: R2.
25. Jonsson, M. V., P. Szodoray, S. Jellestad, et al. 2005. Association between circulating levels of the novel TNF family members APRIL and BAFF and lymphoid organization in primary Sjogren's syndrome. *J. Clin. Immunol*. 25: 189–201.
26. Szyszko, E. A., K. Skarstein, R. Jonsson, and K. A. Brokstad. 2011. Distinct phenotypes of plasma cells in spleen and bone marrow of autoimmune NOD.B10.H2b mice. *Autoimmunity* 44: 415–426.
27. Skarstein, K., A. H. Nerland, M. Eidsheim, et al. 1997. Lymphoid cell accumulation in salivary glands of autoimmune MRL mice can be due to impaired apoptosis. *Scand. J. Immunol*. 46: 373–378.
28. Jonsson, R., A. Tarkowski, K. Backman, et al. 1987. Sialadenitis in the MRL-l mouse: morphological and immunohistochemical characterization of resident and infiltrating cells. *Immunology* 60: 611–616.
29. Jonsson, M. V., N. Delaleu, K. A. Brokstad, et al. 2006. Impaired salivary gland function in NOD mice: association with changes in cytokine profile but not with histopathologic changes in the salivary gland. *Arthritis Rheum*. 54: 2300–2305.
30. Dorner, T., and A. Radbruch. 2007. Antibodies and B cell memory in viral immunity. *Immunity* 27: 384–392.
31. Manz, R. A., A. E. Hauser, F. Hiepe, and A. Radbruch. 2005. Maintenance of serum antibody levels. *Annu. Rev. Immunol*. 23: 367–386.

32. Tew, J. G., R. M. DiLosa, G. F. Burton, et al. 1992. Germinal centers and antibody production in bone marrow. *Immunol. Rev.* 126: 99–112.
33. Jonsson, R., A. Tarkowski, and L. Klareskog. 1986. A demineralization procedure for immunohistopathological use. EDTA treatment preserves lymphoid cell surface antigens. *J. Immunol. Methods*. 88: 109–114.
34. Winter, O., K. Moser, E. Mohr, et al. 2010. Megakaryocytes constitute a functional component of a plasma cell niche in the bone marrow. *Blood*. 116: 1867–1875.
35. Nahar, N. N., S. E. Tague, J. Wang, et al. 2013. Histological characterization of bone marrow in ectopic bone, induced by devitalized Saos-2 human osteosarcoma cells. *Int. J. Clin. Exp. Med*. 6: 119–125.
36. Belnoue, E., C. Tougne, A. F. Rochat, et al. 2012. Homing and adhesion patterns determine the cellular composition of the bone marrow plasma cell niche. *J. Immunol*. 188: 1283–1291.
37. Minges Wols, H. A., G. H. Underhill, G. S. Kansas, and P. L. Witte. 2002. The role of bone marrow-derived stromal cells in the maintenance of plasma cell longevity. *J. Immunol*. 169: 4213–4221.
38. Hjelmstrom, P., J. Fjell, T. Nakagawa, et al. 2000. Lymphoid tissue homing chemokines are expressed in chronic inflammation. *Am. J. Pathol*. 156: 1133–1138.
39. Gatumu, M. K., K. Skarstein, A. Papandile, et al. 2009. Blockade of lymphotoxin-beta receptor signaling reduces aspects of Sjogren's syndrome in salivary glands of non-obese diabetic mice. *Arthritis Res. Ther.* 11: R24.
40. Manzo, A., S. Bugatti, R. Caporali, et al. 2007. CCL21 expression pattern of human secondary lymphoid organ stroma is conserved in inflammatory lesions with lymphoid neogenesis. *Am. J. Pathol*. 171: 1549–1562.
41. Manzo, A., S. Paoletti, M. Carulli, et al. 2005. Systematic microanatomical analysis of CXCL13 and CCL21 *in situ* production and progressive lymphoid organization in rheumatoid synovitis. *Eur. J. Immunol*. 35: 1347–1359.
42. Aqrawi, L. A., K. A. Brokstad, K. Jakobsen, et al. 2012. Low number of memory B cells in the salivary glands of patients with primary Sjogren's syndrome. *Autoimmunity.* 45: 547–555.
43. Sanderson, R. D., P. Lalor, and M. Bernfield. 1989. B lymphocytes express and lose syndecan at specific stages of differentiation. *Cell. Regul*. 1: 27–35.
44. Iwata, Y., Matsushita, T., Horikawa, M., et al. 2011. Characterization of a rare IL-10-competent B-cell subset in humans that parallels mouse regulatory B10 cells. *Blood*. 117: 530–541.
45. Xiao, Y., Hendriks, J., Langerak, P., et al. 2004. CD27 is acquired by primed B cells at the centroblast stage and promotes germinal center formation. *J. Immunol*. 172: 7432–7441.
46. Manz, R. A., A. Thiel, and A. Radbruch. 1997. Lifetime of plasma cells in the bone marrow. *Nature*. 388: 133–134.
47. Tiburzy, B., M. Szyska, H. Iwata, et al. 2013. Persistent autoantibody-production by intermediates between short-and long-lived plasma cells in inflamed lymph nodes of experimental epidermolysis bullosa acquisita. *PLoS One* 8: e83631.

Supplementary material available online
Supplementary Figure S1